

# Sequential Monte Carlo for Sampling Balanced and Compact Redistricting Plans\*

Cory McCartan<sup>†</sup>      Kosuke Imai<sup>‡</sup>

November 13, 2021

## Abstract

Random sampling of graph partitions under constraints has become a popular tool for evaluating legislative redistricting plans. Analysts detect partisan gerrymandering by comparing a proposed redistricting plan with an ensemble of sampled alternative plans. For successful application, sampling methods must scale to large maps with many districts, incorporate realistic legal constraints, and accurately sample from a selected target distribution. Unfortunately, most existing methods struggle in at least one of these three areas. We present a new Sequential Monte Carlo (SMC) algorithm that draws representative redistricting plans from a realistic target distribution of choice. Because it yields nearly independent samples, the SMC algorithm can efficiently explore the relevant space of redistricting plans than the existing Markov chain Monte Carlo algorithms that yield dependent samples. Our algorithm can simultaneously incorporate several constraints commonly imposed in real-world redistricting problems, including equal population, compactness, and preservation of administrative boundaries. We validate the accuracy of the proposed algorithm by using a small map where all redistricting plans can be enumerated. We then apply the SMC algorithm to evaluate the partisan implications of several maps submitted by relevant parties in a recent high-profile redistricting case in the state of Pennsylvania. Open-source software is available for implementing the proposed methodology.

**Key Words:** gerrymandering, graph partition, importance sampling, spanning trees

---

\*We thank Ben Fifield, Greg Herschlag, Mike Higgins, Chris Kenny, Jonathan Mattingly, Justin Solomon, and Alex Tarr for helpful comments and conversations. Imai thanks Yunkyoo Sohn for his contributions at an initial phase of this project. Open-source software is available for implementing the proposed methodology (Fifield et al., 2020c).

<sup>†</sup>Ph.D. student, Department of Statistics, Harvard University. 1 Oxford Street, Cambridge 02138. Email: [cmccartan@g.harvard.edu](mailto:cmccartan@g.harvard.edu)

<sup>‡</sup>Professor, Department of Government and Department of Statistics, Harvard University. 1737 Cambridge Street, Institute for Quantitative Social Science, Cambridge 02138. Email: [imai@harvard.edu](mailto:imai@harvard.edu), URL: <https://imai.fas.harvard.edu/>

# 1 Introduction

In first-past-the-post electoral systems, legislative districts serve as the fundamental building block of democratic representation. In the United States, congressional redistricting, which redraws district boundaries in each state following decennial Census, plays a central role in influencing who is elected and hence what policies are eventually enacted. Because the stakes are so high, redistricting has been subject to intense political battles. Parties often engage in *gerrymandering* by manipulating district boundaries in order to amplify the voting power of some groups while diluting that of others.

In recent years, the availability of granular data about individual voters has led to sophisticated partisan gerrymandering attempts that cannot be easily detected. At the same time, many scholars have focused their efforts on developing methods to uncover gerrymandering by comparing a proposed redistricting plan with a large collection of alternative plans that satisfy the relevant legal requirements. A primary advantage of such an approach over the use of simple summary statistics is its ability to account for idiosyncrasies of physical and political geography specific to each state.

For its successful application, a sampling algorithm for drawing alternative plans must (1) scale to large maps with thousands of geographic units and many districts, (2) simultaneously incorporate a variety of real-world legal constraints such as population balance, geographical compactness, and the preservation of administrative boundaries, and (3) yield a large number of plans that are as independent of one another as possible and are representative of a specific target population, against which a redistricting plan of interest can be evaluated. Although some have been used in several recent court challenges to existing redistricting plans, existing algorithms run into limitations with regards to at least one of these three key requirements.

Optimization-based (e.g., [Mehrotra et al., 1998](#); [Macmillan, 2001](#); [Bozkaya et al., 2003](#); [Liu et al., 2016](#)) and constructive Monte Carlo (e.g., [Cirincione et al., 2000](#); [Chen and Rodden, 2013](#); [Magleby and Mosesson, 2018](#)) methods can be made scalable and incorporate many constraints. But they are not designed to sample from any specific target distribution over redistricting plans. As a result, the resulting plans tend to differ systematically, for example, from a uniform distribution under certain constraints, as [Cho and Liu \(2018\)](#) and [Fifield et al. \(2020a,b\)](#) have found. The absence of an explicit target distribution makes it difficult to interpret the ensembles generated by these methods and use them for statistical outlier analysis to detect gerrymandering.

MCMC algorithms (e.g., [Mattingly and Vaughn, 2014](#); [Wu et al., 2015](#); [Chikina et al., 2017](#); [DeFord et al., 2019](#); [Carter et al., 2019](#); [Fifield et al., 2020a](#)) are in theory able to sample from a specific target distribution, and can incorporate constraints through the use of an energy function. In practice, however, many existing algorithms struggle to mix and traverse through a highly complex sampling space, making scalability difficult and

accuracy hard to prove. Some of these algorithms make proposals by flipping precincts at the boundary of existing districts (e.g., [Mattingly and Vaughn, 2014](#); [Fifield et al., 2020a](#)), rendering it difficult to transition between points in the state space, especially as more constraints are imposed. More recent algorithms by [DeFord et al. \(2019\)](#) and [Carter et al. \(2019\)](#) use spanning trees to make their proposals, and this has allowed these algorithms to yield more global moves and improve mixing. Yet the very essence of the MCMC approach is to generate dependent samples, and on large-scale problems, the dependence in existing algorithms may lead to low efficiency.

In Sections 3 and 4, we present a new Sequential Monte Carlo (SMC) algorithm, ([Doucet et al., 2001](#)) based on a similar spanning tree construction to [DeFord et al. \(2019\)](#) and [Carter et al. \(2019\)](#), that addresses the above three key challenges. Unlike optimization-based and constructive Monte Carlo methods, the SMC algorithm samples from a specific and customizable target distribution. Our algorithm scales better than MCMC algorithms because it generates near-independent samples while directly incorporating the three most common constraints imposed on the redistricting process—contiguity, population balance, and geographic compactness. SMC also removes the need to monitor convergence and mixing, which are essential for the successful application of MCMC algorithms.

The proposed algorithm proceeds by splitting off one district at a time, building up the redistricting plan piece by piece (see [Figure 3](#) for an illustration). Each split is accomplished by drawing a spanning tree and removing one edge, which splits the spanning tree in two. We also extend the SMC algorithm so that it preserves administrative boundaries and certain geographical areas as much as possible, which is another common constraint considered in many real-world redistricting cases. An open-source software package is available for implementing the proposed algorithm ([Fifield et al., 2020c](#)).

In [Section 5](#), we validate the SMC algorithm using a 50-precinct subset of the Florida map, for which all potential redistricting plans can be enumerated ([Fifield et al., 2020b](#)). We demonstrate that the proposed algorithm samples accurately from a range of target distributions on these plans. [Section 6](#) applies the SMC algorithm to the 2011 Pennsylvania congressional redistricting, which was subject to a 2017 court challenge, and compares its performance on this problem with two state-of-the-art MCMC approaches. [Section 7](#) concludes and discusses directions for future work. We now introduce the Pennsylvania case, which serves as our motivating empirical application.

## 2 Empirical Application: The 2011 Pennsylvania Congressional Redistricting

We study the 2011 Pennsylvania congressional redistricting because it illustrates the salient features of the redistricting problem. We begin by briefly summarizing the background of this case and then explain the role of sampling algorithms used in the expert witness reports.

## 2.1 Background

Pennsylvania lost a seat in Congress during the reapportionment of the 435 U.S. House seats which followed the 2010 Census. In Pennsylvania, the General Assembly, which is the state's legislative body, draws new congressional districts, subject to gubernatorial veto. At the time, the General Assembly was controlled by Republicans, and Tom Corbett, also a Republican, served as governor. In the 2012 election, which took place under the newly adopted 2011 districting map, Democrats won 5 House seats while Republicans took the remaining 13. This result stands in sharp contrast to a 7–12 split after the 2010 election as well as a 12–7 Democratic advantage before 2010.

In June 2017, the League of Women Voters of Pennsylvania filed a lawsuit alleging that the 2011 plan adopted by the Republican legislature violated the state constitution by diluting the political power of Democratic voters. The case worked its way through the state court system, and on January 22, 2018, the Pennsylvania Supreme Court issued its ruling, writing that the 2011 plan “clearly, plainly and palpably violates the Constitution of the Commonwealth of Pennsylvania, and, on that sole basis, we hereby strike it as unconstitutional” ([League of Women Voters v. Commonwealth, 2018](#)).

The court ordered that the General Assembly adopt a remedial plan and submit it to the governor, who would in turn submit it to the court, by February 15, 2018. In case no plan was submitted to and approved by that deadline, the court provided that all of the parties to the lawsuit could submit their own plans by the same date, and the court would review them and itself impose a final remedial plan. In its ruling, the court laid out specific requirements that must be satisfied by all proposed plans:

any congressional districting plan shall consist of: congressional districts composed of compact and contiguous territory; as nearly equal in population as practicable; and which do not divide any county, city, incorporated town, borough, township, or ward, except where necessary to ensure equality of population.

While the compactness and administrative boundary constraints are not required for congressional districts by the U.S. or Pennsylvania constitutions, they have been historically held up as “guiding principles” in many states and as a result were explicitly imposed by the court in this case.

The leaders of the Republican Party in the General Assembly drew a new map, but the Democratic governor, Tom Wolf, refused to submit it to the court, claiming that it, too, was an unconstitutional gerrymander. Instead, the court received remedial plans from seven parties: the petitioners, the League of Women Voters; the respondents, the Republican leaders of the General Assembly; the governor, a Democrat; the lieutenant governor, also a Democrat; the Democratic Pennsylvania House minority leadership; the Democratic Pennsylvania Senate minority leadership; and the intervenors, which included Republican party

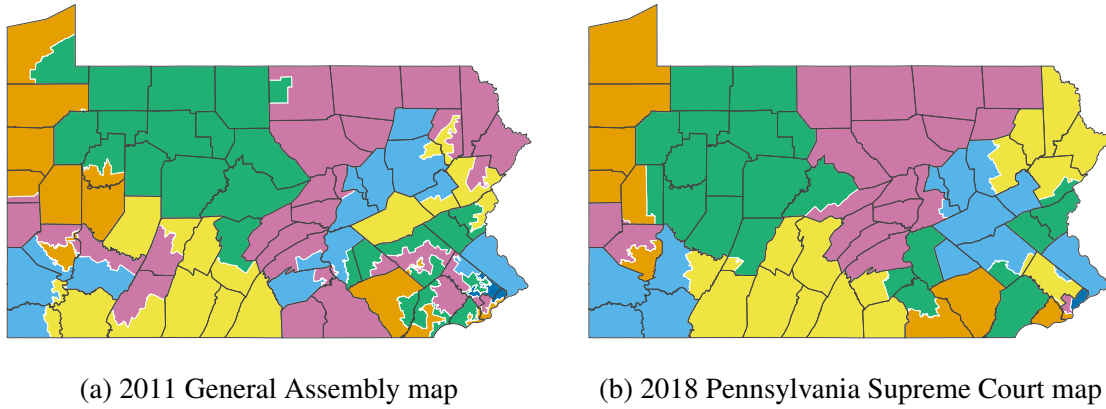


Figure 1: Comparison of the 2011 map drawn by the General Assembly and the final map imposed by the Supreme court in 2018. County lines are shown in dark gray, and district boundaries that do not coincide with county boundaries are in white.

candidates and officials. Ultimately, the Supreme Court drew its own plan and adopted it on February 19, 2018, arguing that it was “superior or comparable to all plans submitted by the parties.” Figure 1 shows the remedial plan created by the Supreme Court as well as the 2011 map adopted by the General Assembly, which were found on the court’s case page.

The constraints explicitly laid out by the court, as well as the numerous remedial plans submitted by the parties, make the 2011 Pennsylvania redistricting a useful case study that evaluates redistricting plans using sampling algorithms.

## 2.2 The Role of Sampling Algorithms

The original finding that the 2011 General Assembly plan was a partisan gerrymander was in part based on different outlier analyses performed by two academic researchers, Jowei Chen and Wesley Pegden, who served as the petitioner’s expert witnesses. [Chen \(2017\)](#) randomly generated two sets of 500 redistricting plans according to a constructive Monte Carlo algorithm based on [Chen and Rodden \(2013\)](#). He considered population balance, contiguity, compactness, avoiding county and municipal splits, and, in the second set of 500, avoiding pairing off incumbents. [Pegden \(2017\)](#) ran an MCMC algorithm for one trillion steps, and computed upper bounds of  $p$ -values using the method of [Chikina et al. \(2017\)](#). This method was also used in a follow-up analysis by Moon Duchin, who served as an expert for the governor ([Duchin, 2018](#)). Both petitioner experts concluded that the 2011 plan was an extreme outlier according to compactness, county and municipal splits, and the number of Republican and Democratic seats implied by various statewide election results.

The respondents also retained several academic researchers as their expert witnesses. One of them, Wendy Tam Cho, directly addressed the sampling-based analyses of Chen and Pegden. [Cho \(2017\)](#) criticized Chen’s analysis for not sampling from a specified target distribution. She also criticized Pegden’s analysis by arguing that his MCMC algorithm only

made local explorations of the space of redistricting plans, and could not therefore have generated a representative sample of all valid plans (see also [Cho and Rubinstein-Salzedo, 2019](#), and the reply by [Chikina et al. \(2019\)](#)). We do not make judgements about the merits of the specific arguments put forth by these expert witnesses. However, these methodological debates that arose in the Pennsylvania case are also relevant for other cases where simulation algorithms have been extensively used by expert witnesses (see e.g., [Rucho v. Common Cause, 2019](#); [Common Cause v. Lewis, 2019](#); [Covington v. North Carolina, 2017](#); [Harper v. Lewis, 2020](#), and the references in [Fifield et al. \(2020b\)](#)).

The expert witness reports in the Pennsylvania case highlight the difficulties in practically applying existing sampling algorithms to actual redistricting problems. First, the distributions that some of these algorithms sample from are not made explicit, leaving open the possibility that the generated ensemble is systematically different from the true set of all valid plans. Second, even when the distribution is known, the Markov chains used to sample from it may be prohibitively slow to mix and therefore cannot guarantee a representative sample. These challenges motivate us to design an algorithm that generates near-independent samples from a specific target distribution and incorporates most common redistricting constraints, while minimizing the impact on scalability, theoretical validity, and empirical performance.

### 3 Sampling Balanced and Compact Districts

In this section, we formally characterize the target distribution of our sampling algorithm. Our goal is to sample redistricting plans with contiguous districts which are both balanced in population and geographically compact.

#### 3.1 The Setup

Redistricting plans are ultimately aggregations of geographic units such as counties, voting precincts, or Census blocks. The usual requirement that the districts in a plan be contiguous necessitates consideration of the spatial relationship between these units. The natural mathematical structure for this consideration is a graph  $G = (V, E)$ , where  $V = \{v_1, v_2, \dots, v_m\}$  consists of  $m$  nodes representing the geographic units of redistricting and  $E$  contains edges connecting units which are legally adjacent.<sup>1</sup>

A redistricting plan on  $G$  consisting of  $n$  districts is described by a function  $\xi : V \rightarrow \{1, 2, \dots, n\}$ , where  $\xi(v) = i$  implies that node  $v$  is in district  $i$ . We let  $V_i(\xi)$  and  $E_i(\xi)$  denote the nodes and edges contained in district  $i$  under a given redistricting plan  $\xi$ , so  $G_i(\xi) = (V_i(\xi), E_i(\xi))$  represents the induced subgraph that corresponds to district  $i$  under the plan. We sometimes suppress the dependence on  $\xi$  when this is clear from context, writing  $G_i = (V_i, E_i)$ . Since each node belongs to one and only one district, we have

---

<sup>1</sup>Depending on the state, two units may be legally adjacent if they have in common a single point, a line segment, or if they are otherwise designated adjacent (as may be the case for islands and the mainland).



$V = \bigcup_{i=1}^n V_i(\xi)$  and  $V_i(\xi) \cap V_{i'}(\xi) = \emptyset$  for any redistricting plan  $\xi$ . In addition, we require that all nodes of a given district be connected.

Beyond connectedness, redistricting plans are almost always required to have nearly equal population in every district. To formalize this requirement, let  $\text{pop}(v)$  denote the population of node  $v$ . Then the population of a district is given by

$$\text{pop}(V_i) := \sum_{v \in V_i(\xi)} \text{pop}(v).$$

We quantify the discrepancy between a given plan and this ideal by the *maximum population deviation* of the plan,

$$\text{dev}(\xi) := \max_{1 \leq i \leq n} \left| \frac{\text{pop}(V_i)}{\text{pop}(V)/n} - 1 \right|,$$

where  $\text{pop}(V)$  denotes the total population. Some courts and states have imposed hard maximums on this quantity, e.g.,  $\text{dev}(\xi) \leq D = 0.05$  for state legislative redistricting.

The proposed algorithm samples plans by way of spanning trees on each district, i.e., subgraphs of  $G_i(\xi)$  which contain all vertices, no cycles, and are connected. Let  $T_i$  represent a spanning tree for district  $i$  whose vertices and edges are given by  $V_i(\xi)$  and a subset of  $E_i(\xi)$ , respectively. The collection of spanning trees from all districts together form a spanning forest  $F = (T_1, \dots, T_n)$ . Each spanning forest implies a redistricting plan where  $\xi(F)(v) = i$  for all  $v \in T_i$ . However, a single redistricting plan may correspond to multiple spanning forests because each district may have more than one spanning tree.

For a given redistricting plan, we can compute the exact number of spanning forests in polynomial time using the determinant of a submatrix of the graph Laplacian, according to the Matrix Tree Theorem of Kirchhoff (see [Tutte \(1984\)](#)). Thus, for a graph  $H$ , if we let  $\tau(H)$  denote the number of spanning trees on the graph, we can represent the number of spanning forests that correspond to a redistricting plan  $\xi$  as

$$\tau(\xi) := \prod_{i=1}^n \tau(G_i(\xi)).$$

This fact will play an important role in the definition of our sampling algorithm and its target distribution, as we explain next.

### 3.2 The Target Distribution

The algorithm is designed to sample a plan  $\xi$  with probability

$$\pi(\xi) \propto \exp\{-J(\xi)\} \tau(\xi)^\rho \mathbf{1}_{\{\xi \text{ connected}\}} \mathbf{1}_{\{\text{dev}(\xi) \leq D\}}, \quad (1)$$

where the indicator functions ensure that the plans meet population balance and connectedness criteria,  $J$  encodes additional constraints on the types of plans preferred, and  $\rho \in \mathbb{R}_0^+$  is chosen to control the compactness of the generated plans. As done in [Section 6](#), we often

use a reasonably strict population constraint such as  $D = 0.001$ . But, in the event that no such constraint exists,  $D$  can be set to  $n - 1$ , which is its maximum value, rendering the constraint moot.

The generality of the additional constraint function  $J$  is intentional, as the exact form and number of additional constraints imposed on the redistricting process varies by state and by the type of districts being drawn. Hard constraints, such as requiring that a certain number of majority-minority districts exist, may be realized by setting  $J(\xi) = 0$  for valid plans, and  $J(\xi) = \infty$  for plans that violate the constraints. Softer constraints may be incorporated by choosing a  $J$  which is small for preferred plans and large otherwise.

For example, a preference for plans that are close to an existing plan  $\xi_{\text{sq}}$  may be encoded by using

$$J_{\text{sq}}(\xi) = -\frac{\beta}{n \log n} \sum_{i=1}^n \sum_{j=1}^n \frac{\text{pop}(V_i(\xi) \cap V_j(\xi_{\text{sq}}))}{\text{pop}(V_j(\xi_{\text{sq}}))} \log \left( \frac{\text{pop}(V_i(\xi) \cap V_j(\xi_{\text{sq}}))}{\text{pop}(V_j(\xi_{\text{sq}}))} \right),$$

where  $\beta \in \mathbb{R}^+$  controls the strength of the constraint. This expression represents the conditional entropy of the distribution of population over the new districts relative to the existing districts, rescaled to  $[0, \beta]$  (Cover and Thomas, 2006). When  $\xi$  is any relabelling of  $\xi_{\text{sq}}$ , then  $J_{\text{sq}}(\xi) = 0$ . In contrast, when  $\xi$  evenly splits the nodes of each district of  $\xi_{\text{sq}}$  between the districts of  $\xi$ , then  $J_{\text{sq}}(\xi) = \beta$ .

If instead we wish to encode a soft preference for plans which split as few administrative units as possible, we could use

$$J_{\text{spl}}(\xi) = \begin{cases} \beta \text{spl}(\xi) & \text{if } \text{spl}(\xi) \leq s_{\text{max}} \\ \infty & \text{otherwise} \end{cases},$$

where  $\text{spl}(\cdot)$  is the number of administrative splits (formally defined in Section 4.5), and  $\beta \in \mathbb{R}^+$  again controls the strength of the soft constraint and  $s_{\text{max}}$  is the maximum number of administrative splits allowed. Examples of other types and formulations of constraints may be found in Bangia et al. (2017), Herschlag et al. (2017), and Fifield et al. (2020a).

Even a small number of constraints incorporated into  $J$  can dramatically limit the number of valid plans and considerably complicate the process of sampling. The Markov chain algorithms developed to date partially avoid this problem by moving toward maps with lower  $J$  over a number of steps, but in general including more constraints makes it even more difficult to transition between valid redistricting plans. Approaches such as simulated annealing (Bangia et al., 2017; Herschlag et al., 2017) and parallel tempering (Fifield et al., 2020a) have been proposed to handle multiple constraints, but these can be difficult to calibrate in practice and provide few, if any, theoretical guarantees.

When only hard constraints are used and  $\rho = 0$  in equation (1), the distribution is uniform across all plans satisfying the constraints. As we will discuss next, larger values of  $\rho$  create a preference for more compact districts;  $\rho = 1$  is a computationally convenient choice which produces satisfactorily compact districts.



### 3.3 Spanning Forests and Compactness

One of the most common redistricting requirements is that districts be geographically compact, though nearly every state leaves this term undefined. Dozens of numerical compactness measures have been proposed, with the Polsby–Popper score (Polsby and Popper, 1991) perhaps the most popular. Defined as the ratio of a district’s area to that of a circle with the same perimeter as the district, the Polsby–Popper score is constrained to  $[0, 1]$ , with higher scores indicating more compactness.

The Polsby–Popper score has been shown to correlate reasonably well with humans’ subjective evaluation of the compactness of districts (Kaufman et al., 2020), but it is far from a perfect measure. One challenge in particular is its sensitivity to the underlying geography and the scale on which it is measured. In states with rugged coastlines or other geographical irregularities, even the most compact districts could have Polsby–Popper scores that are lower than those of gerrymandered districts in other states. And measuring the geography at a 1-meter versus a 1-kilometer scale can shift the Polsby–Popper scores dramatically. This sensitivity makes it difficult to compare the compactness redistricting plans across states, and to set any kind of quantitative standard for the minimum acceptable compactness of legislative districts.

To address this challenge, some scholars have proposed a graph-theoretic measure known as *edge-cut compactness* (Dube and Clark, 2016; DeFord et al., 2019). This measure counts the number of edges that must be removed from the original graph to partition it according to a given plan. Formally, it is defined as

$$\text{rem}(\xi) := 1 - \frac{\sum_{i=1}^n |E_i(\xi)|}{|E(G)|},$$

where we have normalized to the total number of edges.

Plans that involve cutting many edges will necessarily have long internal boundaries, driving up their average district perimeter (and driving down their Polsby–Popper scores), while plans that cut as few edges as possible will have relatively short internal boundaries and much more compact districts. Additionally, given the high density of voting units in urban areas, plans which cut fewer edges will tend to avoid drawing district lines through the heart of these urban areas, since these boundaries will necessarily cut many edges. This has the welcome side effect of avoiding splitting cities and towns, and in doing so helping to preserve “communities of interest,” another common redistricting consideration. The agreement between this measure and the more traditional Polsby–Popper score is clearly visible in Figure 2, which shows the compactness and number of county splits for various maps in the 2011 Pennsylvania congressional redistricting.

Empirically, this graph-based compactness measure tends to be highly correlated with  $\log \tau(G) - \log \tau(\xi)$ . Indeed, in practice, we often observe a correlation in excess of 0.99. It is difficult to precisely characterize this relationship except in special cases because  $\tau(\xi)$

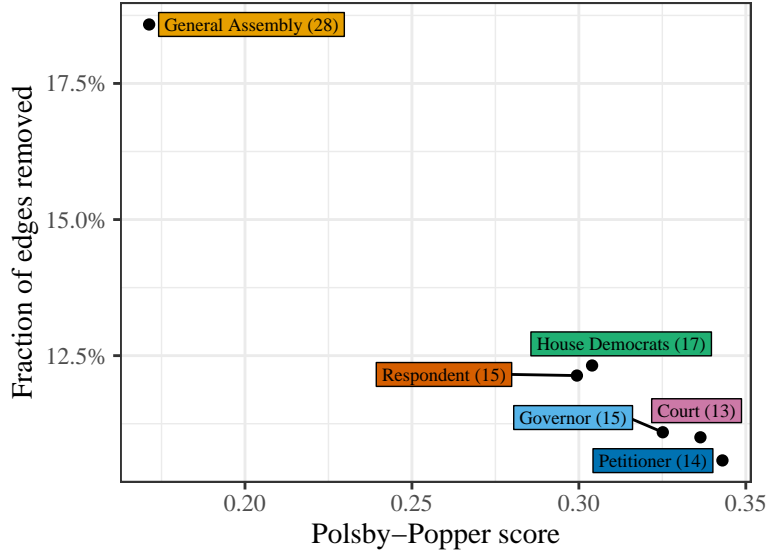


Figure 2: Compactness measures for the six plans from the 2011 Pennsylvania redistricting case. The number of counties split by each plan is given in parentheses within each label.

is calculated as a matrix determinant (McKay, 1981). However, it is well known that this quantity is strongly controlled by the product of the degrees of each node in the graph,  $\prod_{i=1}^m \deg(v_i)$  (Kostochka, 1995). Removing an edge from a graph decreases the degree of the vertices at either end by one, so we would expect  $\log \tau(G)$  to change by approximately  $2\{\log \bar{d} - \log(\bar{d} - 1)\}$  with this edge removal, where  $\bar{d}$  is the average degree of the graph. This implies a linear relation

$$\log \tau(G) - \log \tau(\xi) \approx \text{rem}(\xi) \cdot 2\{\log \bar{d} - \log(\bar{d} - 1)\},$$

so  $\tau(\xi)^\rho \propto \exp(-C \rho \text{rem}(\xi))$ , where  $C$  is an arbitrary constant.

As a result, a greater value of  $\rho$  in the target distribution corresponds to a preference for fewer edge cuts and therefore a redistricting plan with more compact districts. This and the considerations given in the literature (Dube and Clark, 2016; DeFord et al., 2019) suggest that the target distribution in equation (1) with  $\rho = 1$  (or another positive value) is a good choice for sampling compact districts. Of course, if another compactness metric is desired, one can simply set  $\rho = 0$  and incorporate the alternative metric into  $J$ .

## 4 The Proposed Algorithm

The proposed algorithm samples redistricting plans by sequentially drawing districts over  $n - 1$  iterations of a splitting procedure. The algorithm begins by partitioning the original graph  $G = (V, E)$  into two induced subgraphs:  $G_1 = (V_1, E_1)$ , which will constitute a district in the final map, and the remainder of the graph  $\tilde{G}_1 = (\tilde{V}_1, \tilde{E}_1)$ , where  $\tilde{V}_1 = V \setminus V_1$  and  $\tilde{E}_1$  consists of all the edges between vertices in  $\tilde{V}_1$ . Next, the algorithm takes  $\tilde{G}_1$  as an input graph and partitions it into two induced subgraphs, one which will become a district

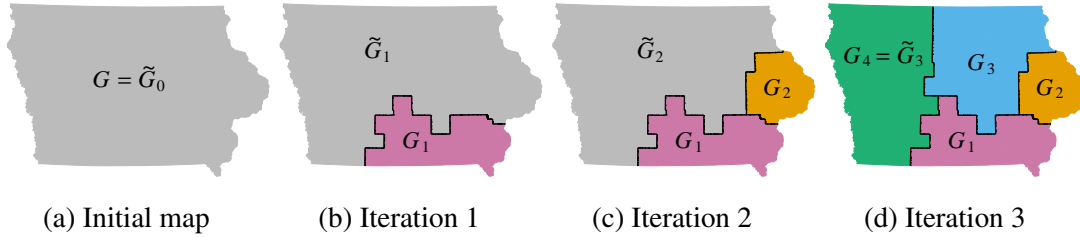


Figure 3: The sequential splitting procedure applied to the state of Iowa, where four congressional districts are created at the county level.

$G_2$  and the remaining graph  $\tilde{G}_2$ . The algorithm repeats the same splitting procedure until the final  $(n - 1)$ -th iteration whose two resulting partitions,  $G_{n-1}$  and  $\tilde{G}_{n-1} = G_n$ , become the final two districts of the redistricting plan.

Figure 3 provides an illustration of this sequential procedure. To independently sample a large number of redistricting plans from the target distribution given in equation (1), at each iteration, the algorithm samples many candidate partitions, discards those which fail to meet the population constraint, and then resamples a certain number of the remainder according to importance weights, using the resampled partitions at the next iteration. The rest of this section explains the details of the proposed algorithm.

#### 4.1 The Splitting Procedure

We first describe the splitting procedure, which is broadly similar to the merge-split Markov chain proposals of DeFord et al. (2019) and Carter et al. (2019). It proceeds by drawing a random spanning tree  $T$ , identifying the  $k_i$  most promising edges to cut within the tree, and selecting one such edge at random to create two induced subgraphs. Spanning trees are an attractive way to split districts, as the removal of a single edge induces a partition which is guaranteed to have two connected components, and spanning trees can be sampled uniformly, using Wilson (1996)’s algorithm.

After splitting, the resulting partition is checked for compliance with the population constraint, by ensuring the population of the new district  $G_i$  falls within the bounds

$$P_i^- = \max \left\{ \frac{\text{pop}(V)}{n}(1 - D), \text{pop}(\tilde{V}_{i-1}) - \frac{n-i}{n} \text{pop}(V)(1 + D) \right\} \quad \text{and}$$

$$P_i^+ = \min \left\{ \frac{\text{pop}(V)}{n}(1 + D), \text{pop}(\tilde{V}_{i-1}) - \frac{n-i}{n} \text{pop}(V)(1 - D) \right\}.$$

These bounds ensure not only that the new district has population deviation below  $D$ , but that it will be possible for future iterations to generate valid districts out of  $\tilde{G}_i$ . If  $\text{pop}(V_i) \notin [P_i^-, P_i^+]$ , then the entire redistricting plan is rejected and the sampling process begins again. While the rate of rejection varies by map and by iteration, we generally encounter acceptance rates between 5% and 30%, which are not so low as to make sampling from large maps intractable. Algorithm 1 details the steps of the splitting procedure, where we take  $\tilde{G}_0 = G$  at the first iteration.

---

**Algorithm 1** Splitting procedure to generate one district

---

*Input:* initial graph  $\tilde{G}_{i-1}$  and a parameter  $k_i \in \mathbb{Z}^+$ .

- (a) Draw a single spanning tree  $T$  on  $\tilde{G}_{i-1}$  uniformly from the set of all such trees using Wilson's algorithm.
- (b) Each edge  $e \in E(T)$  divides  $T$  into two components,  $T_e^{(1)}$  and  $T_e^{(2)}$ . For each edge, compute the following population deviation for the two districts that would be induced by cutting  $T$  at  $e$ ,

$$d_e^{(1)} = \left| \frac{\sum_{v \in T_e^{(1)}} \text{pop}(v)}{\text{pop}(V)/n} - 1 \right| \quad \text{and} \quad d_e^{(2)} = \left| \frac{\sum_{v \in T_e^{(2)}} \text{pop}(v)}{\text{pop}(V)/n} - 1 \right|.$$

Let  $d_e = \min\{d_e^{(1)}, d_e^{(2)}\}$ , and index the edges in ascending order by this quantity, so that we have  $d_{e_1} \leq d_{e_2} \leq \dots \leq d_{e_{m_i-1}}$ , where  $m_i = |V_i|$ .

- (c) Select one edge  $e^*$  uniformly from  $\{e_1, e_2, \dots, e_{k_i}\}$  and remove it from  $T$ , creating a spanning forest  $(T_{e^*}^{(1)}, T_{e^*}^{(2)})$  which induces a partition  $(G_i^{(1)}, G_i^{(2)})$ .
  - (d) If  $d_{e^*}^{(1)} \leq d_{e^*}^{(2)}$ , i.e., if  $T_{e^*}^{(1)}$  induces a district that is closer to the optimal population than  $T_{e^*}^{(2)}$  does, set  $G_i = G_i^{(1)}$  and  $\tilde{G}_i = G_i^{(2)}$ ; otherwise, set  $G_i = G_i^{(2)}$  and  $\tilde{G}_i = G_i^{(1)}$ .
  - (e) If  $\text{pop}(V_i) \in [P_i^-, P_i^+]$ , continue on to the next iteration. Otherwise, reject this map and begin the entire sampling process anew.
- 

## 4.2 The Sampling Probability

The above sequential splitting procedure does not generate plans from the target distribution  $\pi$ . We denote the sampling measure—including the rejection procedure—by  $q$ , and write the sampling probability (for a given connected plan  $\xi$ ) as

$$q(\xi) = q(G_1, G_2, \dots, G_n) = q(G_{n-1} \mid \tilde{G}_{n-2}) \cdots q(G_2 \mid \tilde{G}_1) q(G_1 \mid \tilde{G}_0), \quad (2)$$

where we have used the fact that each new district  $G_i$  depends only on the leftover map area  $\tilde{G}_{i-1}$  from the previous iteration.

The sampling probability at each iteration can be written as the probability that we cut an edge along the boundary of the new district, integrated over all spanning trees which could be cut to form the district, i.e.,

$$q(G_i \mid \tilde{G}_{i-1}) = \sum_{T \in \mathcal{T}(\tilde{G}_{i-1})} q(G_i \mid T) \tau(\tilde{G}_{i-1})^{-1}, \quad (3)$$

where  $\mathcal{T}(\cdot)$  represents the set of all spanning trees of a given graph, and we have relied on the fact that Wilson's algorithm draws spanning trees uniformly.

The key that allows us to calculate  $q(G_i \mid T)$  is that for certain choices of  $k_i$  (the number of edges considered to be cut at iteration  $i$ ), the probability that an edge is cut is

independent of the trees that are drawn. Let  $ok(T)$  represent the number of edges on any spanning tree  $T$  that induce balanced partitions with population deviation below  $D$ , i.e.,

$$ok(T) := |\{e \in E(T) : d_e \leq D\}|.$$

Then define  $K_i := \max_{T \in \mathcal{T}(\tilde{G}_{i-1})} ok(T)$ , the maximum number of such edges across all spanning trees. Furthermore, let  $\mathcal{C}(G, H)$  represent the set of edges joining nodes in a graph  $G$  to nodes in a graph  $H$ . We then have the following result, whose proof appears in Appendix A.

**Proposition 1.** *The probability of sampling a connected redistricting plan  $\xi$  induced by  $\{G_i, \tilde{G}_i\}_{i=1}^{n-1}$ , using parameters  $\{k_i\}_{i=1}^{n-1}$  with  $k_i \geq K_i$ , is*

$$q(\xi) \propto \mathbf{1}_{\{\text{dev}(\xi) \leq D\}} \frac{\tau(\xi)}{\tau(G)} \prod_{i=1}^{n-1} k_i^{-1} |\mathcal{C}(G_i, \tilde{G}_i)|.$$

### 4.3 Sequential Importance Sampling

The factored sampling probability in Proposition 1 naturally suggests a sequential importance sampling approach, as described in Liu et al. (2001), to generate (nearly) independent draws from the target distribution, rather than simply resampling or reweighting after the final stage. A sequential approach is also useful in operationalizing the rejection procedure that is used to enforce the population constraint.

The proposed sequential procedure is governed by two parameters,  $\alpha \in (0, 1]$  and  $M_i \in \mathbb{R}^+$ . These parameters have no effect on the target distribution nor the accuracy of the algorithm; rather, they are chosen to maximize the efficiency of sampling (see Section 4.4). To generate  $S$  nearly independent redistricting plans, at each iteration of the splitting procedure  $i \in \{1, 2, \dots, n-1\}$ , we generate  $S_i = \lceil S \cdot M_i \rceil$  plans, discard the invalid plans, and resample  $S_{i+1}$  plans for the next iteration. Algorithm 2 details the steps of the full SMC algorithm.

One last resampling of  $S$  plans using the outputted weights can be performed to generate a final sample. Alternatively, the weights can be used directly to estimate the expectation of some statistics of interest, which are functions of redistricting plans, under the target distribution, i.e.,  $H = \mathbb{E}_\pi(h(\xi))$ , where  $\pi$  is given in equation (1), using the self-normalized importance sampling estimate

$$\hat{H} = \frac{\sum_{j=1}^{S_{n-1}} h(\xi^{(j)}) w^{(j)}}{\sum_{j=1}^{S_{n-1}} w^{(j)}}.$$

We describe the sampled plans as “nearly independent” because, while the trees are drawn and the edges are cut independently, the weights must be normalized before resampling. This normalization introduces some dependency, but it is much smaller than the autocorrelation generally found in MCMC algorithms.

---

**Algorithm 2** Sequential Monte Carlo (SMC) Algorithm
 

---

*Input:* graph  $G$  to be split into  $n$  districts, target distribution parameters  $\rho \in \mathbb{R}_0^+$  and constraint function  $J$ , and sampling parameters  $\alpha \in (0, 1]$ ,  $M_i$ ,  $M_{i+1}$ , and  $k_i \in \mathbb{Z}^+$ , with  $i \in \{1, 2, \dots, n-1\}$ .

- (a) Generate an initial set of  $S_1$  plans  $\{\tilde{G}_0^{(1)}, \tilde{G}_0^{(2)}, \dots, \tilde{G}_0^{(S_1)}\}$ , where each  $\tilde{G}_0^{(j)} := G$ .
- (b) For  $i \in \{1, 2, \dots, n-2\}$ :
- (i) Sample a total of  $S_i = \lceil S \cdot M_i \rceil$  partial plans  $\{(G_i^{(j)}, \tilde{G}_i^{(j)})\}_{j=1}^{S_i}$ , each of which is obtained from one of the plans from the previous iteration  $\{\tilde{G}_{i-1}^{(j)}\}_{j=1}^{S_{i-1}}$  through one iteration of the splitting procedure (Algorithm 1).
  - (ii) Calculate weights
 
$$w_i^{(j)} = \tau(G_i^{(j)})^{\rho-1} \frac{k_i}{|\mathcal{C}(G_i^{(j)}, \tilde{G}_i^{(j)})|}$$
 for the valid plans that are within the population bounds, and set  $w_i^{(j)} = 0$  for invalid plans.
  - (iii) Resample with replacement a new set of  $S_{i+1}$  partial plans  $\{(G_i^{(j)}, \tilde{G}_i^{(j)})\}_{j=1}^{S_{i+1}}$  according to the weights  $(w_i^{(j)})^\alpha$ .
- (c) Sample a total of  $S_{n-1}$  final partial plans  $\{(G_{n-1}^{(j)}, G_n^{(j)})\}_{j=1}^{S_{n-1}}$ , each of which is obtained from one of the plans from the previous iteration  $\{\tilde{G}_{n-2}^{(j)}\}_{j=1}^{S_{n-2}}$  through one more iteration of the splitting procedure (Algorithm 1).

- (d) Calculate final weights

$$w^{(j)} = \exp\{-J(\xi^{(j)})\} \left( \prod_{i=1}^{n-2} w_i^{(j)} \right)^{(1-\alpha)} \left( \tau(G_{n-1}^{(j)}) \tau(\tilde{G}_{n-1}^{(j)}) \right)^{\rho-1} \frac{k_{n-1}}{|\mathcal{C}(G_{n-1}^{(j)}, \tilde{G}_{n-1}^{(j)})|} \quad (4)$$

for the valid plans that are within the population bounds, and set  $w^{(j)} = 0$  for invalid plans.

- (e) Output the  $S_{n-1}$  plans  $\{\xi^{(j)}\}_{j=1}^{S_{n-1}}$ , where  $\xi^{(j)} = (G_1^{(j)}, \dots, G_{n-1}^{(j)}, G_n^{(j)})$ , and the weights  $\{w^{(j)}\}_{j=1}^{S_{n-1}}$ .
- 

The two asymptotically slowest steps of the sampling procedure are computing  $\tau(G_i)$  for every district  $G_i$  and drawing a spanning tree using Wilson's algorithm for each iteration. All other steps, such as computing  $d_e$  and  $|\mathcal{C}(G_i^{(j)}, \tilde{G}_i^{(j)})|$ , are linear in the number of vertices, and are repeated at most once per iteration.<sup>2</sup> Computing  $\tau(G_i)$  requires computing a determinant, which currently has computational complexity  $O(|V_i(\xi)|^{2.373})$ .<sup>3</sup> Since this

---

<sup>2</sup>To compute  $d_e$ , we walk depth-first over the tree and store, for each node, the total population of that node and the nodes below it. This allows for  $O(1)$  computation of  $d_e$  for all edges.

<sup>3</sup>Though most implementations are  $O(|V_i(\xi)|^3)$ .



must be done for each district of size roughly  $m/n$ , the total complexity is  $O(n \cdot (m/n)^{2.373})$ . For the spanning trees, the expected runtime of Wilson’s algorithm is the mean hitting time of the graph, which is  $O(m^2)$  in the worst case. Since we sample a smaller and smaller tree each iteration, the total complexity is then

$$\sum_{i=1}^{n-1} O\left(\frac{n-i}{n} \cdot m\right)^2 = O(nm^2)$$

So the total complexity for each sample is  $O(nm^2 + m^{2.373}n^{-1.373})$ . Note that when  $\rho = 1$ , we need not compute  $\tau(G_i)$ , and the total complexity is  $O(nm^2)$ .

We confirm the validity of the proposed algorithm by showing that it will generate valid redistricting plans with probability approximately proportional (up to weight normalization error) to the target distribution. This probability may be computed as the product of the splitting procedure sampling probability (Proposition 1) and the importance sampling weights:

$$\begin{aligned} & q(\xi^{(j)})w^{(j)} \prod_{i=1}^{n-2} w_i^{(j)} \\ &= q(\xi^{(j)} \mid \text{dev}(\xi^{(j)}) \leq D) \exp\{-J(\xi^{(j)})\} \tau(G_n^{(j)})^{\rho-1} \prod_{i=1}^{n-1} w_i^{(j)} \\ &\propto \mathbf{1}_{\{\text{dev}(\xi) \leq D\}} \exp\{-J(\xi^{(j)})\} \frac{\tau(\xi^{(j)})}{\tau(G)} \tau(G_n^{(j)})^{\rho-1} \prod_{i=1}^{n-1} k_i^{-1} |\mathcal{C}(G_i^{(j)}, \tilde{G}_i^{(j)})| \cdot \frac{\tau(G_i^{(j)})^{\rho-1} k_i}{|\mathcal{C}(G_i^{(j)}, \tilde{G}_i^{(j)})|} \\ &\propto \exp\{-J(\xi^{(j)})\} \tau(\xi^{(j)})^\rho \mathbf{1}_{\{\text{dev}(\xi) \leq D\}} \\ &= \pi(\xi^{(j)}). \end{aligned}$$

In some cases, the constraints incorporated into  $J(\xi)$  admit a natural decomposition to the district level as  $\prod_{i=1}^n J'(G_i)$ —for example, a preference for districts which split as few counties as possible, or against districts which would pair off incumbents. In these cases, an extra term of  $\exp\{-J'(G_i^{(j)})\}$  can be added to the weights  $w_i^{(j)}$  in each stage, and the same term can be dropped from the final weights  $w^{(j)}$ . This can be particularly useful for more stringent constraints; incorporating  $J'$  in each stage allows the importance resampling to “steer” the set of redistricting plans towards those which are preferred by the constraints.

As regards the parameters, larger values of  $\alpha$  are more aggressive in pruning out unlikely plans (those which are overrepresented in  $q$  versus  $\pi$ ), which may lead to less diversity in the final sample, while smaller values of  $\alpha$  are less aggressive, which can result in more variable final weights and more wasted samples. Liu et al. (2001) recommend a default choice of  $\alpha = 0.5$ ; we find that smaller values such as  $\alpha = 0.1$  may be appropriate for some maps.

Finally,  $M_i$  should be chosen so that out of  $S_i$  plans there are approximately  $S$  valid plans. Doing so minimizes the loss in efficiency incurred by rejecting maps which fail to

meet the population constraints. We will discuss this point in more detail below, as it relates to the choice of  $k_i$ .

## 4.4 Implementation Details

The sequential importance sampling algorithm described above samples from the target distribution given in equation (1), but to practically apply it to non-trivial real-world redistricting problems, there remain several important considerations about its implementation. We first address the choice of  $k_i$ , since  $K_i$  is typically unknown. We also discuss the choice of  $M_i$  and then the stabilization of importance weights for efficient sampling when  $\rho \neq 1$ .

### 4.4.1 Choosing $k_i$

The accuracy of the algorithm is theoretically guaranteed only when the number of edges considered for removal at each stage is at least the maximum number of edges across all graphs which induce districts  $G_i$  with  $\text{dev}(G_i) \leq D$ , i.e.,  $k_i \geq K_i$ . Unfortunately,  $K_i$  is almost always unknown in practice. If we set  $k_i = m - 1$ , where  $m$  represents the total number of nodes in the graph, then this condition is certainly satisfied. However, such a choice results in a prohibitively inefficient algorithm—the random edge selected for removal will with high probability induce an invalid partition, leading to a rejection of the entire map. Conversely, if we set  $k_i = 1$ , we gain efficiency by maximizing the chance that the induced districts satisfy the constraint, but lose the theoretical guarantee.

A natural approach is to draw a moderate number of spanning trees  $\mathcal{T}_i \subseteq \mathcal{T}(\tilde{G}_i)$  and compute  $ok(T)$  for each  $T \in \mathcal{T}_i$ . The sample maximum, or the sample maximum plus some small buffer amount, would then be an estimate of the true maximum  $\hat{K}_i$  and an appropriate choice of  $k_i$ .

In practice, we find that there is little noticeable loss in algorithmic accuracy even if  $k_i < K_i$ , the justification for which is found in the following result. As above,  $d_e$  represents the population deviation of the district induced by removing edge  $e$  from a spanning tree.

**Proposition 2.** *The probability that an edge  $e$  is selected to be cut at iteration  $i$ , given that the tree  $T$  containing  $e$  has been drawn, and that  $e$  would induce a valid district, satisfies*

$$\max \left\{ 0, q(d_e \leq d_{e_{k_i}} \mid \mathcal{F}) \left( 1 + \frac{1}{k_i} \right) - 1 \right\} \leq q(e = e^* \mid \mathcal{F}) \leq \frac{1}{k_i},$$

where  $\mathcal{F} = \sigma(\{T, \text{pop}(V_i) \in [P_i^-, P_i^+]\})$ .

The proof is deferred to Appendix A. If  $k_i \geq K_i$ , then  $q(e = e^* \mid \mathcal{F})$  is exactly  $k_i^{-1}$ , a fact which is used in the proof of Proposition 1. This result, which is proved using a simple Fréchet bound, shows that as long as  $q(d_e \leq d_{e_{k_i}} \mid \mathcal{F})$  is close to 1, using  $k_i^{-1}$  in Proposition 1 is a good approximation to the true sampling probability.

Having sampled  $\mathcal{T}_i$ , we can compute for each value of  $k$  the sample proportion of trees where a randomly selected edge  $e$  among the top  $k$  of edges of the tree is also among the

top  $k$  for the other trees—in effect estimating  $q(d_e \leq d_{e_{k_i}} \mid \mathcal{F})$ . We may then choose  $k_i$  to be the smallest  $k$  for which this proportion exceeds a pre-set threshold (of, say, 0.95 or 0.99). We have found that this procedure, repeated at the beginning of each sampling stage, is an efficient way to select  $k_i$  which does not compromise the ability of the algorithm to sample from the target distribution.

#### 4.4.2 Choosing $M_i$

Once  $k_i$  has been selected, we can reuse the sampled  $\mathcal{T}_i$  to choose  $M_i$ , the oversampling multiplier. We estimate the probability that a randomly chosen edge  $e$  on a spanning tree will have  $d_e \leq D$  as

$$\hat{p} = \sum_{j=0}^{k_i} \frac{j}{k_i} \cdot \frac{|\{T \in \mathcal{T}_i : ok(T) = j\}|}{|\mathcal{T}_i|} = \frac{1}{|\mathcal{T}_i|} \sum_{T \in \mathcal{T}_i} \frac{ok(T)}{k_i}.$$

We then use  $M_i = 1/\hat{p}$  so that out of  $S_i = \lceil S \cdot M_i \rceil$  samples, approximately  $\hat{p} \cdot S_i = S$  are valid. For the final stage, the constraint imposed by  $\text{pop}(V_i) \in [P_i^-, P_i^+]$  can be much more stringent than  $d_e \leq D$  for some maps, and it may be necessary to set  $M_i = c/\hat{p}$  with  $c > 1$  in order to generate enough samples. Although not pursued here, it may also be possible to choose  $M_i$  dynamically by resampling and splitting one map at a time until  $S$  plans are obtained.

#### 4.4.3 Stabilizing importance weights

When  $\rho \neq 1$  or when the constraints imposed by  $J$  are particularly severe, there can be substantial variance in the importance sampling weights. For large maps with  $\rho = 0$ , for instance, since  $\log \tau(\xi) \propto \text{rem}(\xi)$ , the weights will generally span hundreds if not thousands of orders of magnitude. This reflects the general computational difficulty in sampling uniformly from constrained graph partitions. As [Najt et al. \(2019\)](#) show, sampling of node-balanced graph partitions is computationally intractable in the worst case. In such cases, the importance sampling estimates will be highly variable, and resampling based on these weights may lead to degenerate samples with only one unique map.

When the importance weights are variable but not quite so extreme, we find it useful to truncate the normalized weights (such that their mean is 1) from above at a value  $w_{\max}$  before resampling. The theoretical basis for this maneuver is provided by [Ionides \(2008\)](#), who proved that as long as  $w_{\max} \rightarrow \infty$  and  $w_{\max}/S \rightarrow 0$  as  $S \rightarrow \infty$ , the resulting estimates are consistent and have bounded variance. One such choice we have found to work well for the weights generated by this sampling process is  $w_{\max} = S^{0.4}/100$ , though for particular maps other choices of exponent and constant multiplier may be superior.

## 4.5 Incorporating Administrative Boundary Constraints

Another very common requirement for redistricting plans is that districts “to the greatest extent possible” follow existing administrative boundaries such as county and municipality

lines.<sup>4</sup> In theory, this constraint can be formulated using a  $J$  function which penalizes maps for every county line crossed by a district. In practice, however, any algorithm that does not explicitly incorporate this constraint into its design will be unlikely to efficiently generate maps which by random chance respect these boundaries, because there are many more ways to draw lines that meander back and forth across administrative boundaries than there are to follow the boundaries exactly.

Fortunately, with a small modification to the proposed algorithm, we can sample redistricting plans proportional to a similar target distribution but with the additional constraint that the number of administrative splits not exceed  $n - 1$ . In most states, the number of administrative units that are considered (such as counties) is much larger than the number of districts  $n$ , so this constraint represents a significant improvement from the baseline algorithm, which can in theory split each unit up to  $n - 1$  times. With this constraint in place it is much easier to incorporate a further preference for fewer administrative splits through the  $J$  function.

Let  $A$  be the set of administrative units, such as counties and municipalities. We can relate these units to the nodes by way of a labeling function  $\eta : V \rightarrow A$  that assigns each node to its corresponding unit. Thus, our modified algorithm works for non-administrative units so long as they can be represented by this labeling function. This function induces an equivalence relation  $\sim_\eta$  on nodes, where  $v \sim_\eta u$  for nodes  $v$  and  $u$  iff  $\eta(v) = \eta(u)$ . If we quotient  $G$  by this relation, we obtain the administrative-level multigraph  $G / \sim_\eta$ , where each vertex is an administrative unit and every edge corresponds to an edge in  $G$  which connects two nodes in different administrative units. With this notation, we can write the number of administrative splits as

$$\text{spl}(\xi) = \left( \sum_{a \in A} \sum_{i=1}^n C(\eta^{-1}(a) \cap \xi^{-1}(i)) \right) - |A|,$$

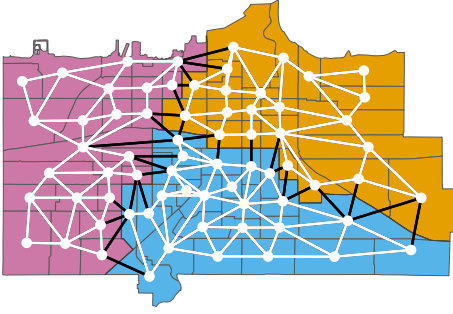
where  $C(\cdot)$  counts the number of connected components in the subgraph  $\eta^{-1}(a) \cap \xi^{-1}(i)$ .

To implement this constraint, we draw the spanning trees in step (a) of the algorithm in two substeps such that we sample from a specific subset of all spanning trees. First, we use Wilson’s algorithm to draw a spanning tree on each administrative unit  $a \in A$ , and then we connect these spanning trees to each other by drawing a spanning tree on the quotient multigraph  $\tilde{G}_i / \sim_\eta$ . Figure 4 illustrates this process and the corresponding graphs. This approach is similar to the independently-developed multi-scale merge-split algorithm of [Autry et al. \(2020\)](#).

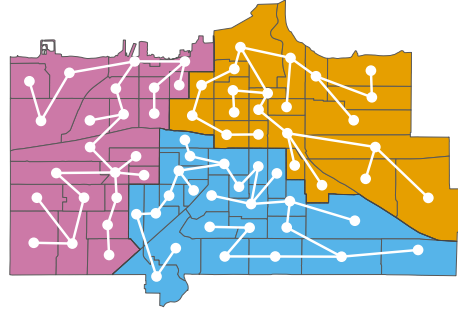
Drawing the spanning trees in two steps limits the trees used to those which, when restricted to the nodes  $\eta^{-1}(a)$  in any administrative unit  $a$ , are still spanning trees. The

---

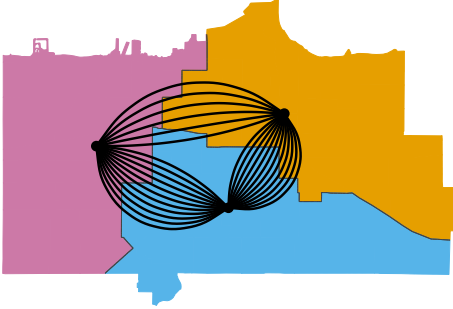
<sup>4</sup>If a redistricting plan must always respect these boundaries, we can simply treat the administrative units as the nodes of the original graph to be partitioned. Here, we consider the preservation of administrative units as a softer constraint.



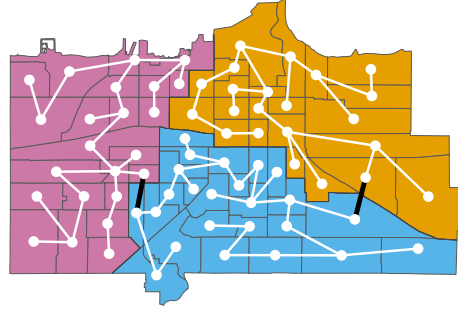
(a) The Erie graph. Edges that cross from one administrative unit to another are colored black.



(b) Spanning trees drawn on each administrative unit.



(c) The quotient multigraph. The number of edges connecting each node is the number of edges that connect each unit in the original graph. We hide self-loops as they are not included in spanning trees.



(d) The final spanning tree, with a spanning tree on the quotient multigraph used to connect the spanning trees on each administrative unit. Notice that removing any edge splits at most one unit.

Figure 4: The two-step spanning tree sampling procedure applied to the city of Erie, Pennsylvania, with three arbitrary administrative units indicated by the colored sections of each map.

importance of this restriction is that cutting any edge in such a tree will either split the map exactly along administrative boundaries (if the edge is on the quotient multigraph) or split one administrative unit in two and preserve administrative boundaries everywhere else. Since the algorithm has  $n - 1$  stages, this limits the support of the sampling distribution to maps with no more than  $n - 1$  administrative splits.

This algorithmic modification does not make theoretical analysis intractable. Indeed, the two-step construction makes clear that the total number of such spanning trees is given by

$$\tau_\eta(\tilde{G}_i) = \tau(\tilde{G}_i / \sim_\eta) \prod_{a \in A} \tau(\tilde{G}_i \cap \eta^{-1}(a)), \quad (5)$$

where  $\tilde{G}_i \cap \eta^{-1}(a)$  denotes the subgraph of  $\tilde{G}_i$  which lies in unit  $a$ , and we take  $\tau(\emptyset) = 1$ . Replacing  $\tau$  with  $\tau_\eta$  in the expression for the weights  $w_i^{(j)}$  and  $w^{(j)}$  then gives the modified algorithm that samples from

$$\pi_\eta(\xi) \propto \exp\{-J(\xi)\} \tau_\eta(\xi)^\rho \mathbf{1}_{\{\xi \text{ connected}\}} \mathbf{1}_{\{\text{dev}(\xi) \leq D\}} \mathbf{1}_{\{\text{spl}(\xi) \leq n-1\}}. \quad (6)$$

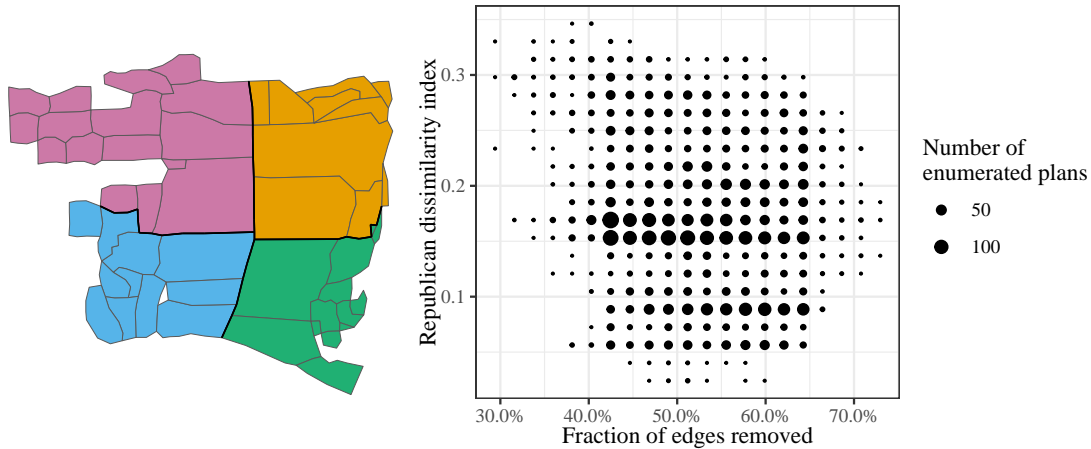


Figure 5: The 50-precinct Florida map used for validation, arbitrarily divided into four administrative units (left), and the joint distribution of Republican dissimilarity and compactness on the map over all partitions into two districts with  $\text{dev}(\xi) \leq 0.05$  (right).

This idea can in fact be extended to arbitrary levels of nested administrative hierarchy. We can, for example, limit not only the number of split counties but also the number of split cities and Census tracts to  $n - 1$  each, since tracts are nested within cities, which are nested within counties. To do so, we begin by drawing spanning trees using Wilson’s algorithm on the smallest administrative units. We then connect spanning trees into larger and larger trees by drawing spanning trees on the quotient graphs of each higher administrative level. Even with multiple levels of administrative hierarchy, the calculation of the number of spanning trees is still straightforward, by analogy to equation (5).

## 5 An Empirical Validation Study

Although the proposed algorithm has desirable theoretical properties, it is important to empirically assess its performance (Fifield et al., 2020b). We examine whether or not the proposed algorithm is able to produce a sample of redistricting maps that is actually representative of a target distribution. We use a 50-precinct map taken from the state of Florida, and use the efficient enumeration algorithm of Fifield et al. (2020b) to obtain a total of 4,266,875 possible redistricting maps with three contiguous districts. We demonstrate that the proposed algorithm can efficiently approximate several target distributions on this set under different sets of constraints.

The left plot of Figure 5 shows this validation map, which we have divided into four arbitrary administrative units. While there are over 4.2 million partitions, only a small number satisfy realistic population and compactness constraints. We sample from three different target measures on the validation map, and compare the samples to the true reference distribution based on the enumeration. When there are only a handful of valid partitions, we directly compare the sample frequency for each partition to the desired uniform distribution. When there are too many partitions to make these individual comparisons, we



compare the samples to the reference enumeration by using the Republican dissimilarity index (Massey and Denton, 1988), a commonly-used measure of spatial segregation. The right plot of the figure shows that with this validation map, the dissimilarity index is particularly sensitive to the compactness of districts. This makes the Republican dissimilarity index a good test statistic for comparing distributions that differ primarily in their average compactness.

We also compare the accuracy of the proposed algorithm to that of the spanning tree-based MCMC algorithm of Carter et al. (2019). This algorithm uses a spanning tree-based proposal similar to the splitting procedure described in Algorithm 1: it merges adjacent districts, draws a spanning tree on the merged district, and splits it to ensure the population constraint is met. Although the parametrization is slightly different, the stationary distribution of this algorithm is exactly that of equation (1). The merge-split algorithm can also incorporate additional constraints into its Metropolis step, but we do not include any here.

It is difficult to directly compare SMC and MCMC algorithms when run for the same number of iterations. SMC samples are nearly independent and require no burn-in period for mixing. In contrast, MCMC samples are generally autocorrelated and require convergence monitoring. The comparisons here are intended to highlight the performance of the two algorithms when run for a moderate but reasonable number of iterations; they are not meant to establish the maximum achievable performance of either algorithm when run under optimal settings.

First, we target a moderately constrained target distribution by choosing  $\rho = 0.5$  in equation (1) and setting the population constraint to  $\text{dev}(\xi) \leq 0.02$ . There are 814 partitions out of 4.2 million (or 0.019% of all maps) that satisfy this population constraint in the reference enumeration. We sampled 10,000 plans using the proposed algorithm and discarded those which did not meet the compactness constraint. We reweighted the remaining 2,995 samples according to the importance weights, using a normalized weight truncation of  $w_{\max} = 0.05 \times \sqrt{10,000}$  (see the lower panel of Figure 6a for the distribution of weights after truncation). We ran the MCMC merge-split algorithm for 20,000 iterations, and discarded the first 10,000 samples. Since the target distribution is no longer uniform, we reweight the enumerated maps according to  $\tau(\xi)^{0.5}$ .

The upper panel of Figure 6a shows the resulting density estimates. While the target distribution is highly multimodal, there is good agreement between the sample and reference distribution. In contrast, the 10,000 samples from the MCMC algorithm fail to accurately capture the left tail of the distribution, and significantly oversample certain values in the right tail.

Second, we target a uniform distribution on the set of maps with  $\text{dev}(\xi) \leq 0.05$  and  $\text{rem}(\xi) \leq 0.35$  — that is, no more than 5% deviation from the population parity and no more than 35% of the edges removed in creating a partition. Note that the median fraction

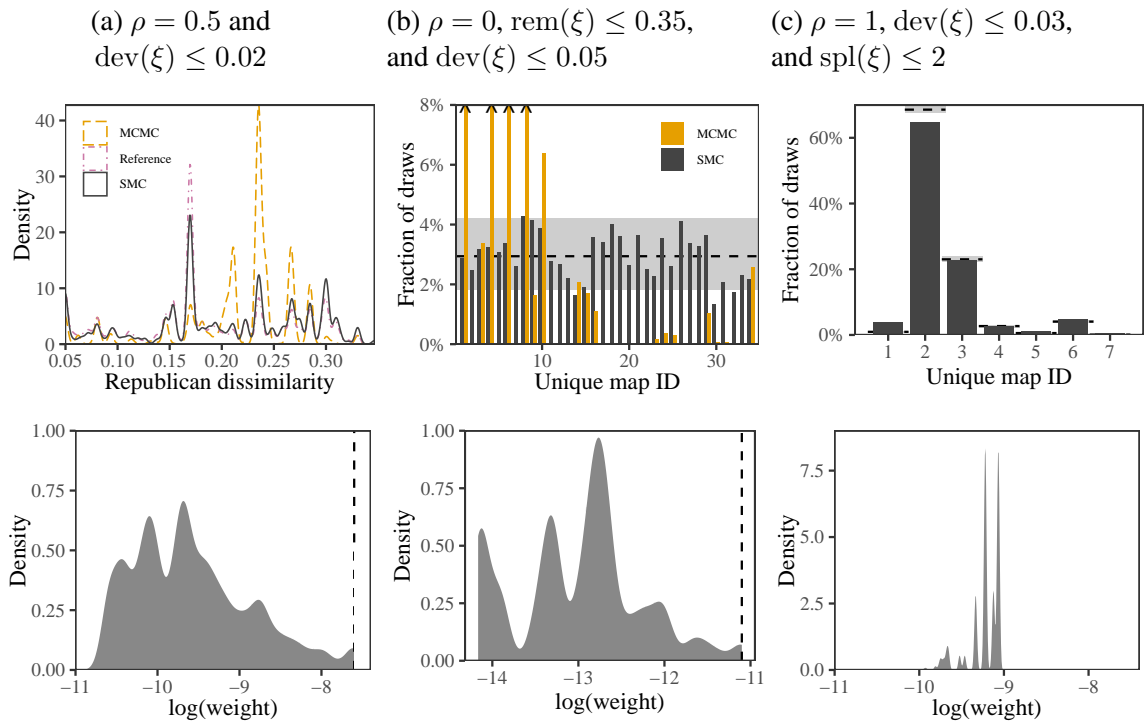


Figure 6: Calibration plots for Republican dissimilarity under various target measures. For target measure (a), density estimates of the the algorithm output and the reweighted enumeration are plotted. For target measures (b) and (c), the sample frequency of individual maps is plotted in gray, with the horizontal line indicating the target frequency and the shaded area indicating the expected range of random variation given the number of effective samples. The distribution of truncated importance weights for each sample is shown below each plot, with the truncation value marked with a vertical line. For target measures (a) and (b), the output of the merge-split MCMC algorithm is also plotted in orange, with values exceeding plot bounds marked with a caret ( $\wedge$ ).

of removed edges across all partitions under 5% population deviation was 53%. There are a total of only 34 maps (or 0.0008% of all maps) that satisfy these two constraints. As before, we sampled 10,000 plans truncate to the same value of  $w_{\max}$  (see the lower panel of Figure 6b for the distribution of truncated weights). We discarded any samples which did not meet the compactness constraint, leaving 2,995 SMC samples and 1,364 MCMC samples.

The upper panel of the figure shows the results. Since there are only 34 maps, we can individually identify each and plot the observed map frequencies versus the expected frequency of  $1/34$ . While the samples do not perfectly approximate the target distribution, the variation in sample frequencies is generally within the range that would be expected due to binomial variation with the number of effective samples obtained here (indicated by a grey band). In comparison, the MCMC algorithm was not able to sample accurately from this target distribution in 20,000 iterations.

Finally, to demonstrate the administrative boundary constraint, we sample from the distribution with  $\rho = 1$ ,  $\text{dev}(\xi) \leq 0.03$ , and  $\text{spl}(\xi) \leq 2$ , using the arbitrary administrative

boundaries shown in the left plot of Figure 5. The combination of these constraints is extremely strong, allowing only at most two county splits. Indeed, only 7 partitions out of over 4.2 million (or approximately 0.00016%) satisfy them all. Since the merge-split MCMC algorithm is not specifically designed to enforce this hard constraint, we do not run it on this target distribution. Instead, we sample 10,000 plans using the modified SMC algorithm of Section 4.5. We do not truncate the weights since with  $\rho = 1$  their variance is quite small, as shown in the lower panel of Figure 6c. As in the second validation exercise, the target measure is not uniform, and the upper panel of Figure 6c plots the sample frequencies of the 7 maps versus their density under the target measure. Despite the severe constraints imposed on the target distribution, the proposed algorithm continues to perform well, although map 1 is oversampled and map 2 is slightly undersampled.

## 6 Empirical Analysis of the 2011 Pennsylvania Redistricting

As discussed in Section 2, in the process of determining a remedial redistricting plan to replace the 2011 General Assembly map, the Pennsylvania Supreme Court received submissions from seven parties. In this section, we compare four of these maps to both the original 2011 plan and the remedial plan ultimately adopted by the court. We study the governor’s plan and the House Democrats’ plan; the petitioner’s plan (specifically, their “Map A”), which was selected from an ensemble of 500 plans used as part of the litigation; and the respondent’s plan, which was drawn by Republican officials. All six plans were within 1 person of equal population across all districts.

### 6.1 The Setup

To evaluate these six plans, we drew 1,500 reference maps from the target distribution given in equation (6) by using the proposed algorithm along with the modifications presented in Section 4.5 to constrain the number of split counties to 17 (out of a total of 67), in line with the court’s mandate. We set  $\rho = 1$  to put most of the sample’s mass on compact districts, and enforced  $\text{dev}(\xi) \leq 0.001$  to reflect the “one person, one vote” requirement. The parameters  $k_i$  and  $M_i$  were selected according to the automated procedures laid out in Sections 4.4.1 and 4.4.2, with a threshold value of 0.95. The average rejection rates at each iteration was 15.1%.

This population constraint translates to a tolerance of around 700 people, in a state where the median precinct has 1,121 people. Like most research on redistricting, we use precincts because they represent the smallest geographical units for which election results are available. To draw from a stricter population constraint we would need to use the 421,545 Census blocks in Pennsylvania rather than the 9,256 precincts, which would significantly increase the computational burden. Given that the error in Census population

totals is likely much greater than 0.1%, we do not believe that our choice of a 0.1% population constraint has a significant impact on our conclusions here.

## 6.2 Comparison with State-of-the-Art MCMC Methods

We first compare the computational performance of the SMC algorithm with two state-of-the-art MCMC methods based on spanning trees.<sup>5</sup> As discussed earlier, the proposed method generates nearly independent samples but it may yield extreme weights. Thus, the relative efficiency between them depends on the distribution of weights for our method and the degree of autocorrelation for MCMC methods.

The first MCMC algorithm is the merge-split procedure of [Carter et al. \(2019\)](#) that was used in Section 5. For this comparison, we set  $\rho = 1$  (in our parametrization), so that the merge-split algorithm and the proposed algorithm are sampling from approximately the same target distribution (the merge-split procedure does not automatically incorporate the hard county split constraint). The second algorithm is the recombination (“ReCom”) proposal of [DeFord et al. \(2019\)](#), which pioneered the spanning tree-based merge-split proposal used in [Carter et al. \(2019\)](#). Although the ReCom algorithm does not ensure that samples are drawn from a particular target distribution, the authors provide empirical evidence that the resulting chains do converge to a (unknown) stationary distribution.

Neither the merge-split algorithm nor the ReCom algorithm are designed to enforce a hard constraint on the number of county splits, though these preferences can be encoded in an energy function. Here, for the sake of comparison, we did not enforce any additional constraints in running either algorithm. Since additional constraints generally lead to substantially less efficiency in MCMC settings, we do not expect this simplification to affect our qualitative findings.

To measure the algorithms’ performance, we draw 1,500 Pennsylvania redistricting maps of 18 districts with  $\text{dev}(\xi) \leq 0.001$  using each algorithm and calculate the number of effective samples. For the MCMC algorithms this is done through the usual autocorrelation-based formula for two summary statistics (see, e.g. [Geyer, 2011](#)): the gerrymandering index (see below for a definition) and the Republican dissimilarity index described above. For the SMC algorithm we use the effective sample calculation for functions of interest given in [Owen \(2013\)](#), which uses the distribution of importance sampling weights.

The results are shown in Table 1. The SMC algorithm is seven to 150 times more efficient than either of the MCMC algorithms. We cannot directly compare these algorithms in terms of their runtime since it depends on specific implementations of each algorithm. An exact theoretical comparison is also difficult. Although the computational complexity for a sample from the SMC algorithm is  $O(nm^2)$  (see Section 4.3), while the complexity

---

<sup>5</sup>We use their open-source implementations, which are available online: ReCom at <https://github.com/mggg/GerryChain> (version 0.2.8, accessed July 30, 2020), and merge-split at <https://git.math.duke.edu/gitlab/gjh/mergesplitcodebase> (accessed July 30, 2020).

	Gerrymandering index			Republican dissimilarity		
	SMC	ReCom	Merge-split	SMC	ReCom	Merge-split
Nominal Samples	1500	1500	1500	1500	1500	1500
Effective samples	580.2	76.0	27.1	859.7	40.2	5.6
Efficiency	38.7%	5.1%	1.8%	57.3%	2.7%	0.4%

Table 1: Comparison of runtime and efficiency of the proposed Sequential Monte Carlo (SMC) algorithm and two state-of-the-art MCMC algorithms with spanning tree-based proposals: ReCom and Merge-split.

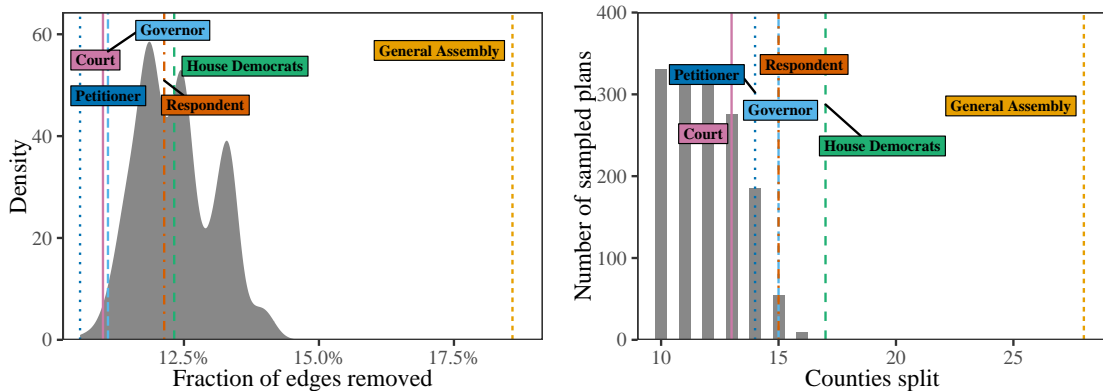


Figure 7: Summary statistics for the six plans, compared to their distribution under the target measure. The left plot shows  $\text{rem}(\xi)$ , where smaller values indicate more compact districts. The right plot shows  $\text{spl}(\xi)$ , whose median value under the target measure is 12.

of the MCMC proposals here is  $O(m^2)$ , the MCMC algorithms only change two districts at a time, whereas an SMC sample redraws all eighteen. For this particular application, the specific implementations of the the SMC, ReCom MCMC, and merge-split MCMC algorithms we used took 140, 46, and 11 minutes to sample, respectively. This implies that SMC is much more effective than the state-of-the-art MCMC algorithms in terms of runtime per effective sample. Although additional study is warranted, our results suggest that the proposed algorithm may be substantially more efficient when applied to real-world redistricting problems.

### 6.3 Compactness and County Splits

Figure 7 shows distribution of the fraction of edges removed ( $\text{rem}(\xi)$ ) and the number of county splits ( $\text{spl}(\xi)$ ) across the reference maps generated by our algorithm (grey histograms). The figure also plots these values for each of the six plans using vertical lines of various types. The 2011 General Assembly plan is a clear outlier for both statistics, being far less compact and splitting far more counties than any of the reference plans and all of the remedial plans. Among the remedial plans, the petitioner’s is the most compact, followed by the court’s and the governor’s, according to the  $\text{rem}(\xi)$  statistic. The House Democratic plan and the respondent’s plan were the least compact based on both statistics,

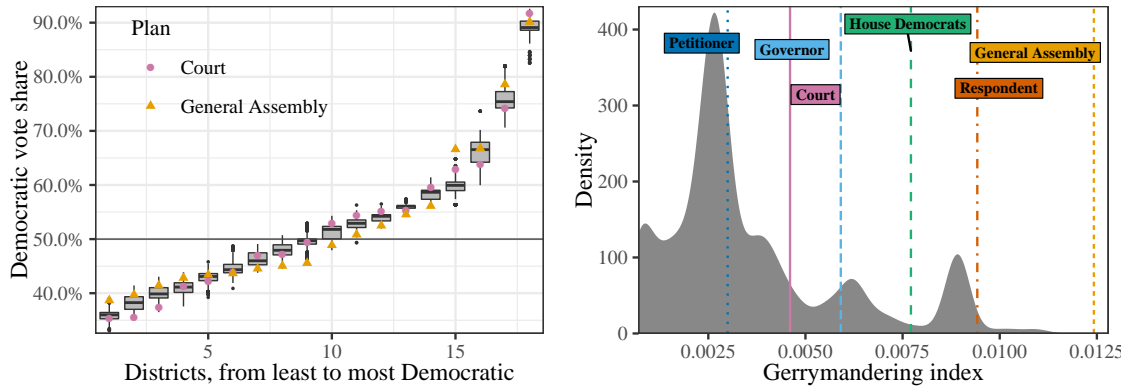


Figure 8: Democratic vote share by districts (left plot), where within each plan districts are ordered by Democratic vote share, and the derived gerrymandering index (right plot), which is computed as the total squared deviation from the mean district-vote share relationship in the left plot.

though still well within the normal range, according to the reference maps. In fact, the petitioner’s plan appears to be an outlier in being *too* compact, although this is perhaps not surprising—the map was generated by an algorithm explicitly designed to optimize over criteria such as population balance and compactness (Chen, 2017).

The right plot of Figure 7 shows that all of the submitted plans split between 13 and 17 counties, with the court’s adopted plan splitting the fewest. Yet around half of the reference maps split fewer than 13 counties, with some splitting only 10. This may be a result of the stricter 0% population constraint met by the six plans, or a different prioritization between the various constraints imposed.

## 6.4 Partisan Analysis

But while important, the outlier status of the General Assembly plan as regards compactness and county splits is not sufficient to show that it is a *partisan* gerrymander. To evaluate the partisan implications of the six plans, we take a precinct-level baseline voting pattern and aggregate it by district to explore hypothetical election outcomes under the six plans and the reference maps. The baseline pattern is calculated by averaging the vote totals for the three presidential elections and three gubernatorial elections that were held in Pennsylvania from 2000 to 2010 (Ansolabehere and Rodden, 2011). We do not use state legislative or congressional election results, as different voters were presented with different candidates. We use election data from 2000 to 2010, as these would have been available at the time of redistricting, and were also the data used during litigation. While being far from a perfect way to create counterfactual election outcomes, this simple averaging of statewide results is often used in academic research and courts. A more thorough analysis might consider each election separately, or try to model the congressional vote accounting for incumbency and other effects.

We begin our partisan analysis by computing the “gerrymandering index” proposed by



[Bangia et al. \(2017\)](#) for the six plans as well as the sampled reference maps. Within each plan, we number the districts by their baseline Democratic vote share, so District 1 is the least Democratic and District 18 the most. The left plot of [Figure 8](#), analogous to [Figure 7](#) in [Herschlag et al. \(2017\)](#), presents the distribution of the Democratic vote share for each of the districts across the reference maps, and also shows the values for the General Assembly plan (orange triangles) and the court's adopted plan (purple circles). We observe that when compared to the reference maps and the court's plan, the General Assembly plan tends to yield smaller Democratic vote share in competitive districts while giving larger Democratic vote share in non-competitive districts. This finding is consistent with the view that the General Assembly plan is gerrymandered in favor of Republicans by packing Democratic voters in non-competitive districts.

From this district-vote share relationship, we can compute the gerrymandering index by summing the squared deviations from the mean vote share in each district. The right plot of [Figure 8](#) shows the distribution of this index based on the reference maps and indicates the values of the six maps. By this metric, the General Assembly plan is a clear outlier, as are the respondent's plan and the House Democrats' plan. The petitioner's plan has the smallest gerrymandering index among the six studied plans, while the plans adopted by the Governor and the court are within the normal range, according to the reference maps.

While the gerrymandering index provides a useful numerical summary of the district-vote share relationship, it weights all deviations equally and does not consider their direction. The structure of these plans and the importance of the location and direction of these deviations become even clearer when we group the districts and sum the deviations from median vote share across the group. Positive deviations within a group indicate that voters in these districts tilt more Democratic than would otherwise be expected, while negative deviations indicate the same for Republicans. [Figure 9](#) shows the results of this grouping, and lays bare the strategy underlying each plan.

The General Assembly plan has outlier deviations for all four groups, clearly packing Democratic voters into safe Republican (1–5) and safe Democratic (15–18) districts, while cracking them and diluting their vote shares in the competitive districts (6–10 and 11–14). The respondent's remedial plan, while not as extreme, maintains the packing in Districts 15–18 and cracking in 6–14. In contrast, the House Democrats' plan tries the opposite tack, cracking Republican voters Districts 11–14 and packing them into the heavily Republican Districts 1–5. Intriguingly, the court's adopted plan has a very similar pattern to the House Democrats' plan, while the petitioner's plan appears to be the most balanced. This may explain the general surprise expressed in the media that Democrats unexpectedly benefited from the court's new plan (see, e.g. [Cohn, 2018](#)).

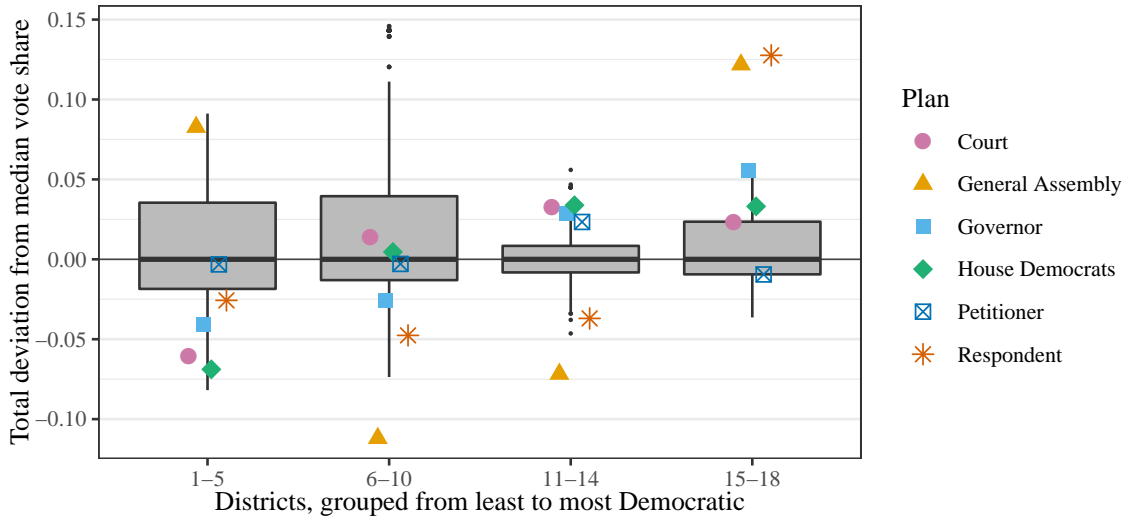


Figure 9: The eighteen districts are put into four groups depending on their Democratic vote share, and the total deviation from the median vote share of each group is plotted for each plan and the reference ensemble. The points are horizontally jittered to improve the visualization without altering their values. Gerrymandering is visible as a pattern of cracking voters in the middle two groups and packing them into the outer groups, diluting their voting power in competitive districts.

## 7 Concluding Remarks

Redistricting sampling algorithms allow for the empirical evaluation of a redistricting plan by generating alternative plans under a certain set of constraints. Researchers and policy-makers can compute various statistics from the redistricting plan of interest and compare them with the corresponding statistics based on these sampled plans. Unfortunately, existing approaches often struggle when applied to real-world problems, owing to the scale of the problems and the number of constraints involved.

The SMC algorithm presented here is able to sample from a specific target distribution, but does not face the same kinds of scalability problems as many existing MCMC algorithms. It also incorporates, by design, the common redistricting constraints of population balance, geographic compactness, and minimizing administrative splits. Additionally, every sample is nearly independent of the others, leading to increased efficiency compared to highly dependent Markov chains and eliminating the concerns about mixing as well as the need to monitor convergence. We expect these advantages of the proposed SMC algorithm to substantially improve the reliability of outlier analysis in real-world redistricting cases.

Future research should explore the possibility of improving several design choices in the algorithm to further increase its efficiency. Wilson’s algorithm, for instance, can be generalized to sample from edge-weighted graphs. Choosing weights appropriately could lead to trees which induce maps that are more balanced or more compact. And the procedure for choosing edges to cut, while allowing for the sampling probability to be calculated,

introduces inefficiencies by leading to many rejected maps. Further improvements in either of these areas should allow us to better sample and investigate redistricting plans over large maps and with even more complex sets of constraints.

Second, little is known about the measure on graph partitions induced by cutting spanning trees. Can we relate properties of the overall graph to the distribution of  $\text{rem}(\xi)$ ? Is a particular choice of  $\rho$  more natural than any other, and does this depend on the graph in question? What is the distribution of  $\tau(\xi)$  (and therefore of the importance weights), and does this converge to any particular distribution as the number of districts or the number of nodes grows? Understanding this measure better should provide more theoretical guarantees and allow researchers to better design and understand target distributions for redistricting sampling.

## A Proofs of Propositions

**Proposition 1.** *The probability of sampling a connected redistricting plan  $\xi$  induced by  $\{G_i, \tilde{G}_i\}_{i=1}^{n-1}$ , using parameters  $\{k_i\}_{i=1}^{n-1}$  with  $k_i \geq K_i$ , is*

$$q(\xi) \propto \mathbf{1}_{\{\text{dev}(\xi) \leq D\}} \frac{\tau(\xi)}{\tau(G)} \prod_{i=1}^{n-1} k_i^{-1} |\mathcal{C}(G_i, \tilde{G}_i)|.$$

*Proof.* We have factored the overall sampling probability in equation (2) and written the sampling probability at each iteration in equation (3).

Any spanning tree can be decomposed into two other trees and an edge joining them. Let  $T \cup e \cup T'$  denote the spanning tree obtained by joining two other spanning trees,  $T$  and  $T'$ , with an edge  $e$ . Then equation (3) can be written as

$$q(G_i | \tilde{G}_{i-1}) = \sum_{\substack{T^{(1)} \in \mathcal{T}(G_i) \\ T^{(2)} \in \mathcal{T}(\tilde{G}_i)}} \sum_{e \in \mathcal{C}(T^{(1)}, T^{(2)})} q(G_i | T^{(1)} \cup e \cup T^{(2)}) \tau(\tilde{G}_{i-1})^{-1}.$$

Now,  $q(G_i | T^{(1)} \cup e \cup T^{(2)})$  is determined by two factors: whether  $e^* = e$ , i.e., if  $e$  is the edge selected to be cut, and whether  $\text{pop}(V_i) \in [P_i^-, P_i^+]$ . If  $\text{pop}(V_i) \notin [P_i^-, P_i^+]$  then the map is rejected and the probability is zero. Therefore

$$q(G_i | T^{(1)} \cup e \cup T^{(2)}) \propto \mathbf{1}_{\{\text{pop}(V_i) \in [P_i^-, P_i^+]\}} q(e^* = e | T^{(1)} \cup e \cup T^{(2)}, \text{pop}(V_i) \in [P_i^-, P_i^+]).$$

What determines if  $e^* = e$ ? If  $e$  has  $d_e$  in the top  $k_i$ , then it has a  $1/k_i$  probability of being selected in step (c) and cut. If  $d_e$  is not in the top  $k_i$ , then this probability is zero.

In addition, notice that the forward-looking bounds  $P_i^-$  and  $P_i^+$  are stricter than merely ensuring  $\text{dev}(G_i) \leq D$ . That is, conditional on  $\text{pop}(V_i) \in [P_i^-, P_i^+]$ , we must have  $\text{dev}(G_i) \leq D$ .

Therefore, if a sorted edge  $e_j$  in any spanning tree induces such a balanced partition, we must have  $j \leq K_i$ , where as above  $K_i$  counts the maximum number of such edges across all possible spanning trees. Thus, so long as we set  $k_i \geq K_i$ , we will have  $d_e \leq D$ .

Furthermore, across all spanning trees  $T^{(1)} \in \mathcal{T}(G_i)$  and  $T^{(2)} \in \mathcal{T}(\tilde{G}_i)$ , and connecting edges  $e \in E(T^{(1)}, T^{(2)})$ , the value of  $d_e$  is constant, since removing  $e$  induces the same districting. Combining these two facts, we have

$$q(e^* = e \mid T^{(1)} \cup e \cup T^{(2)}, \text{pop}(V_i) \in [P_i^-, P_i^+]) = k_i^{-1},$$

which does not depend on  $T^{(1)}$ ,  $T^{(2)}$ , or  $e$ . We may therefore write the sampling probability as

$$\begin{aligned} q(G_i \mid \tilde{G}_{i-1}) &\propto \sum_{\substack{T^{(1)} \in \mathcal{T}(G_i) \\ T^{(2)} \in \mathcal{T}(\tilde{G}_i)}} \sum_{e \in \mathcal{C}(T^{(1)}, T^{(2)})} \frac{\mathbf{1}_{\{\text{pop}(V_i) \in [P_i^-, P_i^+]\}}}{k_i \tau(\tilde{G}_{i-1})} \\ &= \frac{\tau(G_i) \tau(\tilde{G}_i)}{\tau(\tilde{G}_{i-1}) k_i} |\mathcal{C}(G_i, \tilde{G}_i)| \mathbf{1}_{\{\text{pop}(V_i) \in [P_i^-, P_i^+]\}}, \end{aligned} \quad (7)$$

where as in the main text we let  $\mathcal{C}(G, H)$  represent the set of edges joining nodes in a graph  $G$  to nodes in a graph  $H$ . Substituting equation (7) into equation (2), the factored sampling probability telescopes, and we find

$$\begin{aligned} q(\xi) &= \prod_{i=1}^{n-1} q(G_i \mid \tilde{G}_{i-1}) \\ &\propto \prod_{i=1}^{n-1} \frac{\tau(G_i) \tau(\tilde{G}_i)}{\tau(\tilde{G}_{i-1}) k_i} |\mathcal{C}(G_i, \tilde{G}_i)| \mathbf{1}_{\{\text{pop}(V_i) \in [P_i^-, P_i^+]\}} \\ &= \mathbf{1}_{\{\text{dev}(\xi) \leq D\}} \frac{\tau(\xi)}{\tau(G)} \prod_{i=1}^{n-1} k_i^{-1} |\mathcal{C}(G_i, \tilde{G}_i)|. \quad \square \end{aligned}$$

**Proposition 2.** *The probability that an edge  $e$  is selected to be cut at iteration  $i$ , given that the tree  $T$  containing  $e$  has been drawn, and that  $e$  would induce a valid district, satisfies*

$$\max \left\{ 0, q(d_e \leq d_{e_{k_i}} \mid \mathcal{F}) \left( 1 + \frac{1}{k_i} \right) - 1 \right\} \leq q(e = e^* \mid \mathcal{F}) \leq \frac{1}{k_i},$$

where  $\mathcal{F} = \sigma(\{T, \text{pop}(V_i) \in [P_i^-, P_i^+]\})$ .

*Proof.* We can write

$$q(e = e^* \mid \mathcal{F}) = q(e = e^*, d_e \leq d_{e_{k_i}} \mid \mathcal{F}) = \frac{1}{k_i} q(d_e \leq d_{e_{k_i}} \mid \mathcal{F}),$$

This holds because the edge  $e$  will not be cut unless  $d_e \leq d_{e_{k_i}}$ , i.e., if  $e$  is among the top  $k_i$  edges. We then have immediately that  $q(e = e^* \mid \mathcal{F}) \leq k_i^{-1}$ . Additionally, using the lower Fréchet inequality, we find the lower bound

$$\begin{aligned} q(e = e^* \mid \mathcal{F}) &= q(e = e^*, d_e \leq d_{e_{k_i}} \mid \mathcal{F}) \\ &\geq \max \left\{ 0, q(e = e^* \mid \mathcal{F}) + q(d_e \leq d_{e_{k_i}} \mid \mathcal{F}) - 1 \right\} \\ &= \max \left\{ 0, \frac{1}{k_i} q(d_e \leq d_{e_{k_i}} \mid \mathcal{F}) + q(d_e \leq d_{e_{k_i}} \mid \mathcal{F}) - 1 \right\} \\ &= \max \left\{ 0, q(d_e \leq d_{e_{k_i}} \mid \mathcal{F}) \left( 1 + \frac{1}{k_i} \right) - 1 \right\}. \quad \square \end{aligned}$$

## References

- Ansolabehere, S. and Rodden, J. (2011). Pennsylvania Data Files.
- Autry, E., Carter, D., Herschlag, G., Hunter, Z., and Mattingly, J. (2020). Multi-scale merge-split Markov chain Monte Carlo for redistricting. *Working paper*.
- Bangia, S., Graves, C. V., Herschlag, G., Kang, H. S., Luo, J., Mattingly, J. C., and Ravier, R. (2017). Redistricting: Drawing the line. *arXiv preprint arXiv:1704.03360*.
- Bozkaya, B., Erkut, E., and Laporte, G. (2003). A tabu search heuristic and adaptive memory procedure for political districting. *European journal of operational research*, 144(1):12–26.
- Carter, D., Herschlag, G., Hunter, Z., and Mattingly, J. (2019). A merge-split proposal for reversible Monte Carlo Markov chain sampling of redistricting plans. *arXiv preprint arXiv:1911.01503*.
- Chen, J. (2017). Expert report of Jowei Chen, Ph.D. Expert witness report in League of Women Voters v. Commonwealth.
- Chen, J. and Rodden, J. (2013). Unintentional gerrymandering: Political geography and electoral bias in legislatures. *Quarterly Journal of Political Science*, 8(3):239–269.
- Chikina, M., Frieze, A., and Pegden, W. (2017). Assessing significance in a Markov chain without mixing. *Proceedings of the National Academy of Sciences*, 114(11):2860–2864.
- Chikina, M., Frieze, A., and Pegden, W. (2019). Understanding our Markov Chain significance test: A reply to Cho and Rubinstein-Salzedo. *Statistics and Public Policy*, 6(1):50–53.
- Cho, W. K. T. (2017). Expert report of Wendy K. Tam Cho. Expert witness report in League of Women Voters v. Commonwealth.
- Cho, W. K. T. and Liu, Y. Y. (2018). Sampling from complicated and unknown distributions: Monte Carlo and Markov chain Monte Carlo methods for redistricting. *Physica A: Statistical Mechanics and its Applications*, 506:170–178.
- Cho, W. K. T. and Rubinstein-Salzedo, S. (2019). Understanding significance tests from a non-mixing Markov Chain for partisan gerrymandering claims. *Statistics and Public Policy*, 6(1):44–49.
- Cirincione, C., Darling, T. A., and O’Rourke, T. G. (2000). Assessing South Carolina’s 1990s congressional districting. *Political Geography*, 19(2):189–211.

- Cohn, N. (2018). Democrats didnt even dream of this Pennsylvania map. How did it happen? *The New York Times*.
- Common Cause v. Lewis (2019). 834 S.E.2d 425 (N.C.: Supreme Court).
- Cover, T. M. and Thomas, J. A. (2006). *Elements of information theory*. John Wiley & Sons, 2 edition.
- Covington v. North Carolina (2017). 270 F. Supp. 3d 881 (M.D.N.C.).
- DeFord, D., Duchin, M., and Solomon, J. (2019). Recombination: A family of Markov chains for redistricting. *arXiv preprint arXiv:1911.05725*.
- Doucet, A., de Freitas, N., and Gordon, N., editors (2001). *Sequential Monte Carlo methods in practice*. Springer, New York.
- Dube, M. P. and Clark, J. T. (2016). Beyond the circle: Measuring district compactness using graph theory. In *Annual Meeting of the Northeastern Political Science Association*.
- Duchin, M. (2018). Outlier analysis for pennsylvania congressional redistricting.
- Fifield, B., Higgins, M., Imai, K., and Tarr, A. (2020a). Automated redistricting simulation using Markov chain Monte Carlo. *Journal of Computational and Graphical Statistics*, page Forthcoming.
- Fifield, B., Imai, K., Kawahara, J., and Kenny, C. T. (2020b). The essential role of empirical validation in legislative redistricting simulation. *Statistics and Public Policy*, page Forthcoming.
- Fifield, B., Kenny, C. T., McCartan, C., Tarr, A., and Imai, K. (2020c). *redist*: Computational algorithms for redistricting simulation. Available at the Comprehensive R Archive Network (CRAN). <https://CRAN.R-project.org/package=redist>.
- Geyer, C. (2011). Introduction to Markov chain Monte Carlo. In *Handbook of Markov chain Monte Carlo*, pages 3–48. CRC Press, Boca Raton.
- Harper v. Lewis (2020). No. 5: 19-CV-452-FL (D.N.C.).
- Herschlag, G., Ravier, R., and Mattingly, J. C. (2017). Evaluating partisan gerrymandering in Wisconsin. *arXiv preprint arXiv:1709.01596*.
- Ionides, E. L. (2008). Truncated importance sampling. *Journal of Computational and Graphical Statistics*, 17(2):295–311.



- Kaufman, A., King, G., and Komisarchik, M. (2020). How to measure legislative district compactness if you only know it when you see it. *American Journal of Political Science*, page Forthcoming.
- Kostochka, A. V. (1995). The number of spanning trees in graphs with a given degree sequence. *Random Structures & Algorithms*, 6(2-3):269–274.
- League of Women Voters v. Commonwealth (2018). 178 A. 3d 737 (Pa: Supreme Court).
- Liu, J. S., Chen, R., and Logvinenko, T. (2001). A theoretical framework for sequential importance sampling with resampling. In *Sequential Monte Carlo methods in practice*, pages 225–246. Springer.
- Liu, Y. Y., Cho, W. K. T., and Wang, S. (2016). PEAR: a massively parallel evolutionary computation approach for political redistricting optimization and analysis. *Swarm and Evolutionary Computation*, 30:78–92.
- Macmillan, W. (2001). Redistricting in a GIS environment: An optimisation algorithm using switching-points. *Journal of Geographical Systems*, 3(2):167–180.
- Magleby, D. B. and Mosesson, D. B. (2018). A new approach for developing neutral redistricting plans. *Political Analysis*, 26(2):147–167.
- Massey, D. S. and Denton, N. A. (1988). The dimensions of residential segregation. *Social forces*, 67(2):281–315.
- Mattingly, J. C. and Vaughn, C. (2014). Redistricting and the will of the people. *arXiv preprint arXiv:1410.8796*.
- McKay, B. D. (1981). Spanning trees in random regular graphs. In *Proceedings of the Third Caribbean Conference on Combinatorics and Computing*. Citeseer.
- Mehrotra, A., Johnson, E. L., and Nemhauser, G. L. (1998). An optimization based heuristic for political districting. *Management Science*, 44(8):1100–1114.
- Najt, L., Deford, D., and Solomon, J. (2019). Complexity and geometry of sampling connected graph partitions. *arXiv preprint arXiv:1908.08881*.
- Owen, A. B. (2013). *Monte Carlo theory, methods and examples*, chapter 9, page 12.
- Pegden, W. (2017). Pennsylvanias congressional districting is an outlier: Expert report. Expert witness report in League of Women Voters v. Commonwealth.
- Polsby, D. D. and Popper, R. D. (1991). The third criterion: Compactness as a procedural safeguard against partisan gerrymandering. *Yale Law & Policy Review*, 9(2):301–353.

Rucho v. Common Cause (2019). 139 S. Ct. 2484, 204 L. Ed. 2d 931, 588 U.S.

Tutte, W. T. (1984). *Graph Theory*. Addison-Wesley.

Wilson, D. B. (1996). Generating random spanning trees more quickly than the cover time.  
In *Proceedings of the twenty-eighth annual ACM symposium on Theory of computing*,  
pages 296–303.

Wu, L. C., Dou, J. X., Sleator, D., Frieze, A., and Miller, D. (2015). Impartial redistricting:  
A Markov Chain approach. *arXiv preprint arXiv:1510.03247*.